

Supporting Information for
Conformational Dynamics of Single G Protein-Coupled Receptors in Solution

Samuel Bockenhauer^{1,2,*}, Alexandre Fürstenberg^{1,*^a}, Xiao Jie Yao³, Brian K. Kobilka³, and W. E. Moerner¹

¹ Department of Chemistry, Stanford University, Stanford, CA 94305

² Department of Physics, Stanford University, Stanford, CA 94305

³ Department of Molecular and Cellular Physiology, Stanford University School of Medicine, Stanford, CA 94305

* Equal contributions

^a Present address: Department of Structural Biology and Bioinformatics, University of Geneva, 1211 Genève 4, Switzerland

Spectra and quantum yield calculation

Absorption and fluorescence spectra were recorded on 1-3 μM solutions of $\beta_2\text{AR-TMR}$ in the presence and in the absence of the full agonist BI-167107. Upon agonist binding, no change in extinction coefficient was observed (Figure S1a), but the fluorescence intensity increased (Figure S1b) and the fluorescence spectrum displayed a small hypsochromic shift.

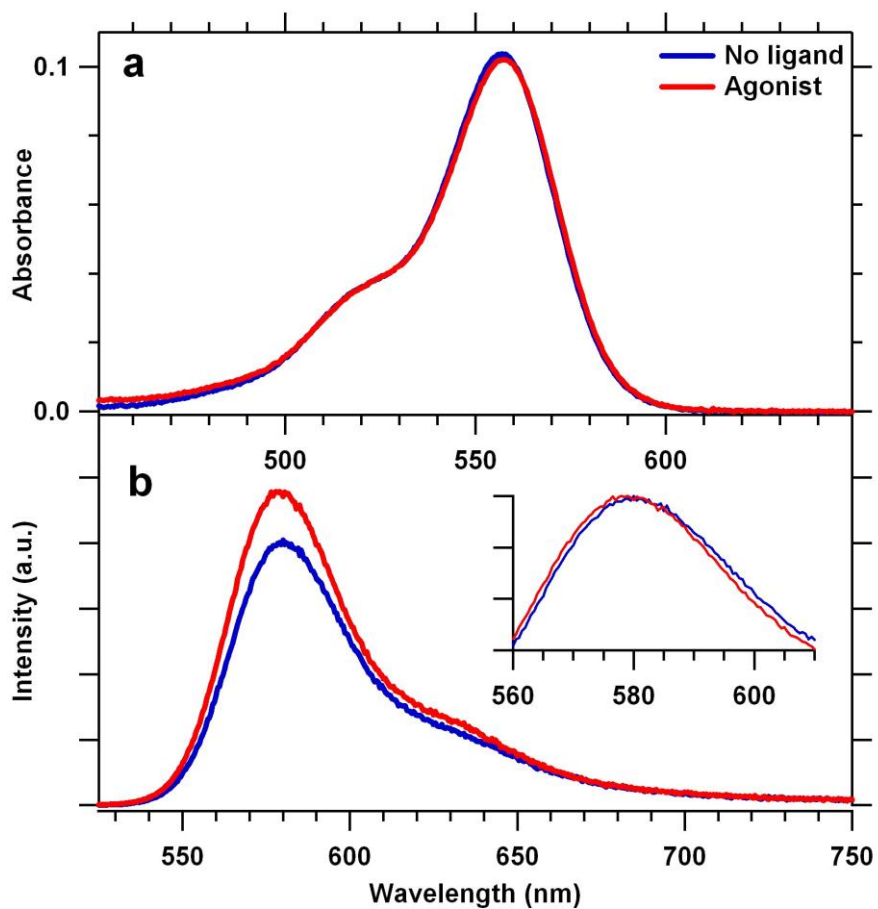


Figure S1. Absorption (a) and fluorescence (b) spectra of β_2 AR-TMR in the presence and in the absence of the full agonist BI-167107. The fluorescence quantum yield increases upon binding of agonist. The inset shows intensity-normalized fluorescence spectra of both samples, demonstrating a weak (4 nm) hypsochromic shift in the presence of agonist.

Single-molecule lifetime fitting

To fit single-molecule lifetimes, an experimental decay function is optimized to fit the data according to the Maximum Likelihood Estimation (MLE) criterion, which is preferred over least-squares fitting for small numbers of photons due to its correct accounting of Poisson noise. In this work, the measured decay for each 10 ms bin and also for each identified intensity state is fitted with the experimental decay function

$$F(t, t_c, \tau, \gamma) = (1 - \gamma) \left[IRF(t) \otimes \exp\left(\frac{-(t - t_c)}{\tau}\right) \right] + \gamma BKG(t)$$

where t is the delay time, t_c is the color shift, τ is the fitted lifetime, $IRF(t)$ is the measured instrument response function, \otimes indicates convolution, γ is the measured background decay fraction, and $BKG(t)$ is the measured background decay. The background decay $BKG(t)$ is calculated from ~ 5 s of hand-selected background in each 300 s data trace during which no receptors are trapped, and the background decay fraction is calculated for each state from a three-parameter fit to $F(t, t_c, \tau, \gamma)$ in which γ is a free parameter. For the lifetime fits in each 10 ms bin, only a two-parameter fit to $F(t, t_c, \tau)$ was used, because γ was already determined with high accuracy from the three-parameter fit to all photons in the state. The lifetime determined from each 10 ms bin allows estimation of the lifetime with higher time resolution than merely pooling all photons from an identified intensity state. Figure S2 demonstrates the ability to resolve evident high-lifetime (left panels) and low-lifetime levels (right panels) within the same identified intensity state.

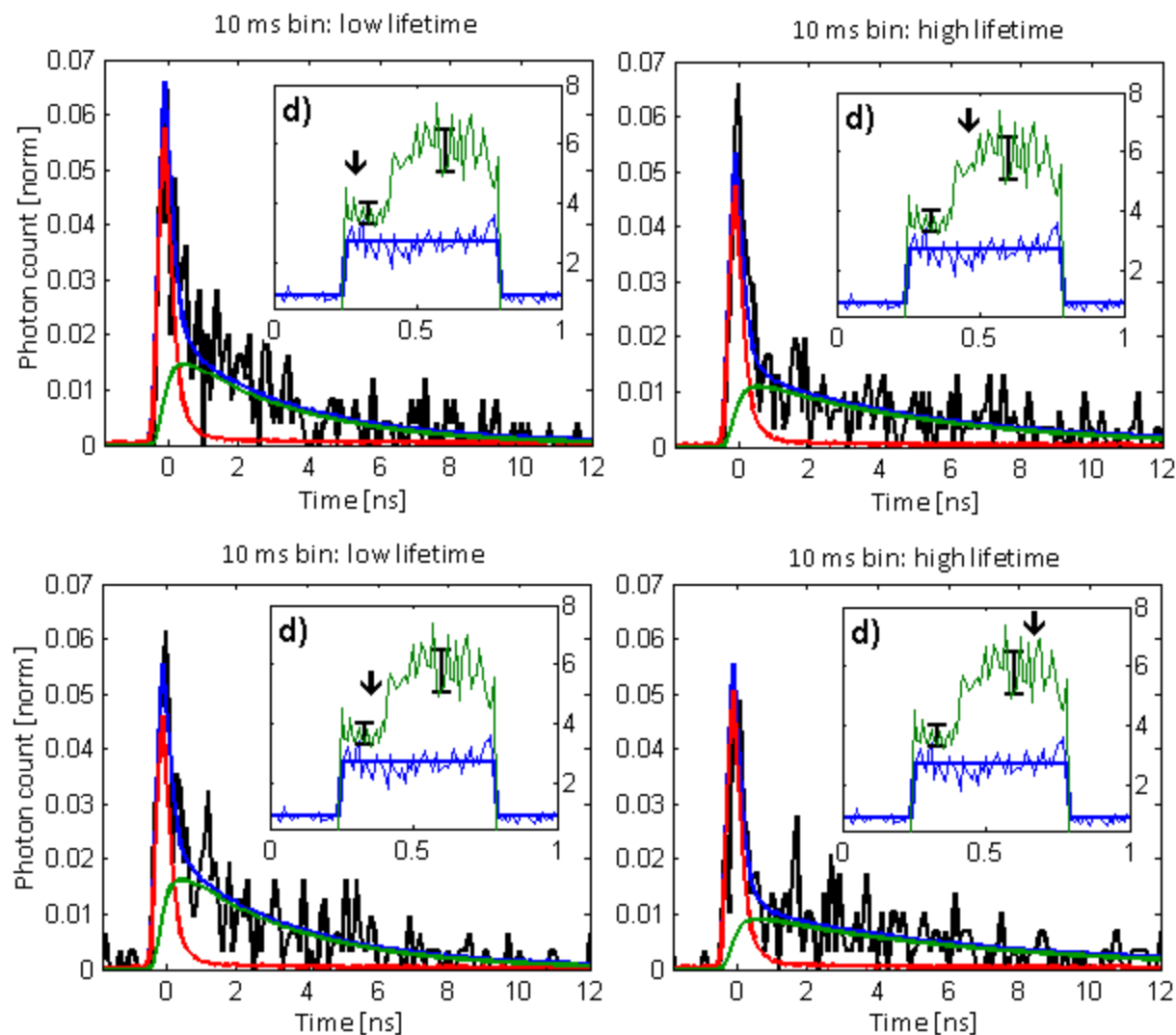


Figure S2. Distinguishing a significant change in lifetime within a single trapped receptor state. We show four typical lifetime decays resulting from only the photons in an individual 10 ms time bin indicated by the arrows (time traces, inset). The inset trapped receptor trace is from Figure 4d. On the decays (black) we overlay the convolved, fitted lifetime component (green), the measured background component (red), and their sum, yielding the total fit (blue). Decays from the low lifetime level (left panels) are clearly distinguishable from those from the high lifetime level (right panels).

Autocorrelation fitting and controls

Intensity autocorrelation allows dynamical description of fluctuations in receptor microenvironment as sensed by TMR. In the ABEL trap, the circularly-revolving excitation beam will introduce a sinusoidal oscillation in the autocorrelation function because the receptor's position at a given time is correlated with its position a short time later, before it can diffuse (or be kicked by the trap) to a new, uncorrelated location. The envelope of this oscillation, however, decays quickly (Figure S3); after several passes of the 26 kHz revolving beam, the receptor's position is uncorrelated with its initial position. To probe intrinsic receptor dynamics, as is our goal, we fit only correlation lags greater than ~ 5 revolution periods = 200 μs .

Figure S4 shows control experiments in which we calculate the intensity autocorrelation of background in the trap and of trapped 20 nm fluorescent polystyrene beads. The flatness of the background autocorrelation proves that on the timescales of interest ($>200 \mu\text{s}$), no artifacts are observed from glass, buffer, or PDMS autofluorescence. The fluorescent beads, pumped at low power, contain many independently-emitting fluorescent labels, and as such we expect no intrinsic fluctuations to be present. Moreover, the triplet state lifetime of TMR under standard conditions is known to be in the $\sim \mu\text{s}$ range, far below our fitted timescale (Geissbuehler et al., *Biophys. J.* 2010, 98, 339-349). The flatness of the autocorrelations for two different trapped beads confirms that the revolving excitation beam does not introduce artifacts in the autocorrelation. These facts justify our interpretation of receptor autocorrelation decays as resulting from intrinsic fluctuations in receptor microenvironment.

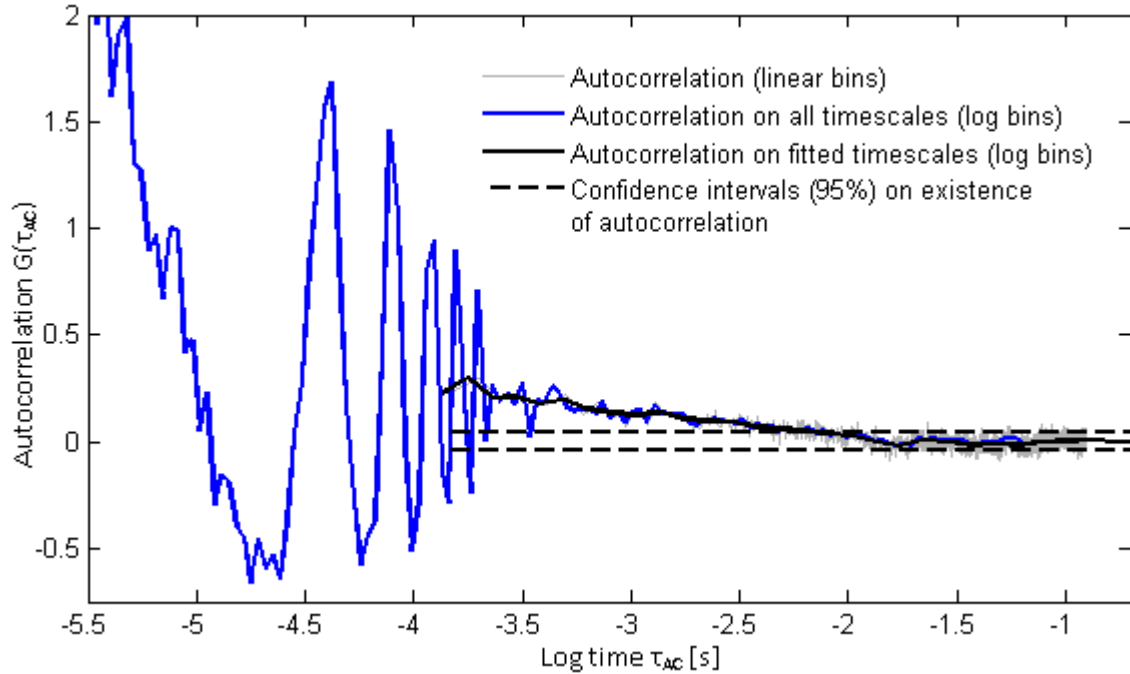


Figure S3. Influence of the circularly-revolving trap beam on the autocorrelations. We re-plot the autocorrelation from Figure 6a with linear bins (gray), logarithmic bins (black), confidence intervals (dashed), and we also include the autocorrelation calculated with logarithmic bins extending down to $\sim 1 \mu\text{s}$ time lag (blue). The expected fast sinusoidal autocorrelation at the modulation frequency dies out at time lags long compared to the modulation period $(26 \text{ kHz})^{-1} = 38 \mu\text{s}$. To avoid any modulation artifacts due to low sampling at short time lags, we fit (as shown) only lags greater than $200 \mu\text{s}$.

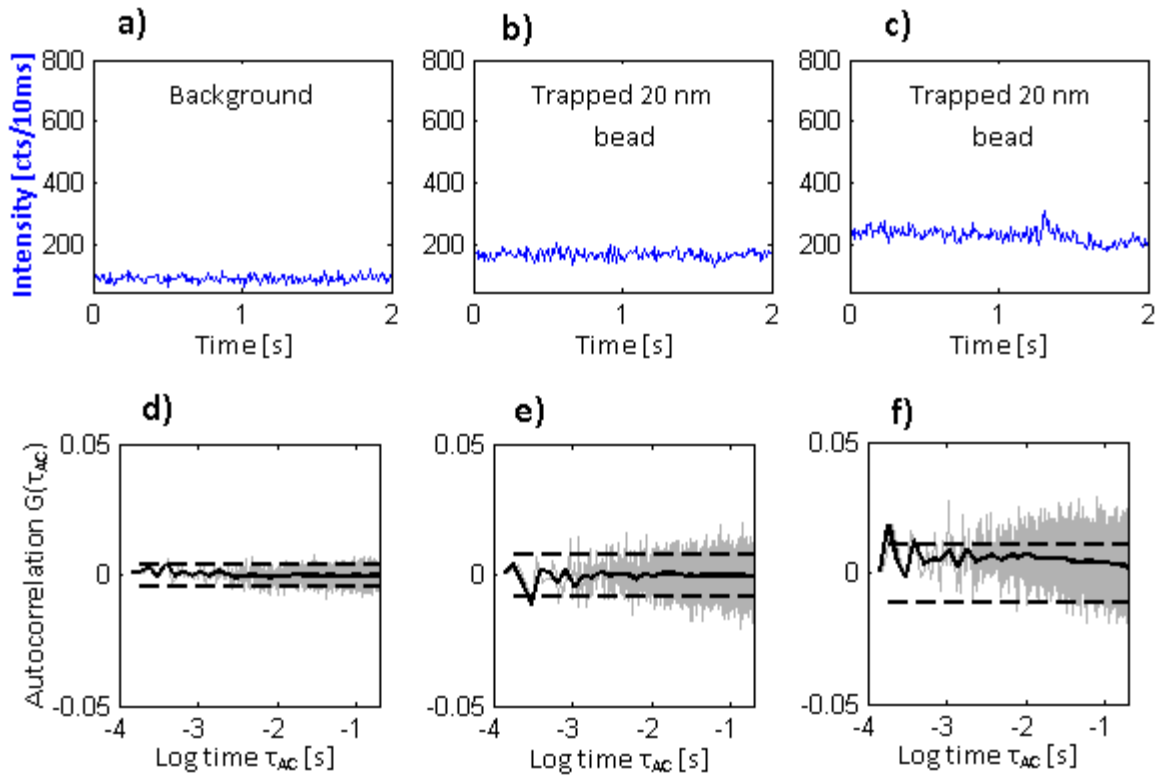


Figure S4. Absence of autocorrelation from background and trapped beads. We show time traces of background in the trap and its autocorrelation (**a,d**), a trapped 20 nm bead and its autocorrelation (**b,e**), and another trapped 20 nm bead and its autocorrelation (**c,f**). All show negligible autocorrelations, even if the time trace shows modest changes in intensity (**c**) due to diffusing impurities or bead-dye photophysics.

Bulk Anisotropy

The fluorescence anisotropy data was fitted with a biexponential model (see main text):

$$r(t) = r_0 \left[a_{r1} \exp\left(-\frac{t}{\tau_{r1}}\right) + a_{r2} \exp\left(-\frac{t}{\tau_{r2}}\right) \right].$$

Lipari and Szabo (Lipari, G.; Szabo, A. *Biophys. J.* **1980**, *30*, 489-506) demonstrate that the fluorescence polarization anisotropy of a probe wobbling within a cone with rotational time constant τ_w as the macromolecule to which it is bound tumbles with rotational constant τ_M can be described by:

$$r(t) = r_0 \left[(1-S) \exp\left(-\frac{t}{\tau_w}\right) + S \right] \exp\left(-\frac{t}{\tau_M}\right) = r_0 \left[(1-S) \exp\left(-\frac{t}{\tau_w} - \frac{t}{\tau_M}\right) + S \exp\left(-\frac{t}{\tau_M}\right) \right],$$

where S is a so-called order parameter related to the semi-angle of the cone explored by the probe. Table S1 shows the resulting wobbling-in-a-cone parameters. In the case of well-separated, decoupled wobbling and tumbling time scales, as is the case here, the results are equivalent to a biexponential model.

Table S1. Parameters describing the fluorescence polarization anisotropy decay of β_2 AR-TMR in the absence and in the presence of BI-167107 using the “wobbling-in-a-cone” model of Lipari and Szabo (Lipari, G.; Szabo, A. *Biophys. J.* **1980**, *30*, 489-506).

Ligand	τ_w (ns)	τ_M (ns)	S	r_0
No ligand	0.8	8.2	0.74	0.38
BI-167107	0.7	30	0.93	0.38